



DETECTING COASTAL FEATURE CHANGES IN THE MEKONG DELTA USING MULTI-TEMPORAL LANDSAT DATA AND GOOGLE EARTH IMAGES

D. Hak¹, K. Nadaoka¹, A. Collin²

¹ Department of Mechanical and Environmental Informatics, Graduate School of Information Science and Engineering, Tokyo Institute of Technology. E-mail: hak.d.aa@m.titech.ac.jp

² Littoral Geomorphology & Environment, Ecole Pratique des Hautes Etudes. E-mail: antoine.collin@ephe.sorbonne.fr

ABSTRACT

Investigating feature coastal changes is a crucial task focusing on the identification of potential factors that trigger the degradation of coastal ecosystems. However, in-situ field investigations can be costly and time-consuming, and are almost impossible for multi-decadal assessments. In this study, the evolution of coastal features (including shoreline patterns and coastal habitats) in KienGiang province, the north-westernmost part of the Mekong Delta, was investigated using multi-temporal Landsat data and high-resolution Google Earth Images (GEIs). The aims of this study are three-fold: (i) to delineate and detect the inter-decadal shoreline evolution based on Landsat data; (ii) to detect coastal land cover changes using Landsat data and GEIs; and (iii) to evaluate the impacts of socio-economic activities on the coastal ecosystem, particularly the mangrove ecosystem. The results of this study revealed that between 1989 and 2014 the shoreline pattern of the study area changed significantly owing to erosion and accretion phenomena driven by intensive human activity along the coastline. The rate of coastal erosion has increased continuously up to the present day, with a shift in the dominant erosion zone from north to south. Also, coastal land cover has significantly and continually changed. The bare surface coverage has decreased remarkably while other land cover types such as urban areas, vegetation cover, and inland water surfaces have continually increased. This reflects the trend of increasing human activity in this coastal region. Moreover, the contrasting variation patterns of paddy areas and inland water surfaces show that the socio-economic situation of the study site has changed from rice-oriented to aquaculture-oriented; this change took place in the early 2000s. The extent of the mangrove forest continuously declined from 1995 onward. The conversion of the adjacent coastal land cover was found to have a potentially negative effect on the degradation of the mangrove area. Moreover, concentrated economic activities such as intensive shrimp breeding and rice cultivation, industrial development, and the increasing number of human inhabitants have resulted in severe damage to the mangrove ecosystem.

Keywords: Remote sensing, Coastal features, Change detection, Impact assessment.

Received 13 March 2015. Accepted 7, June 2015

Presented in IWTC 18th

1 INTRODUCTION

Coastal regions commonly feature extremely rich ecosystems, ranging from coastal wetlands to estuaries and mangrove forests, which provide extensive benefits and economic value, marking them as attractive places for human habitation. Nevertheless, many pristine coastal zones around the world have been altered to fulfill the socio-economic desires of human beings (e.g., the Nile and Mekong deltas). Coastal vegetation, such as the mangrove and other aquatic plants, make an ideal habitat and present abundant food sources for aquatic species (Nagelkerken et al., 2008; Manson et al., 2005). However, overexploitation of coastal ecosystem services to feed a continuously growing population has led to the widespread elimination of natural habitats, including mangrove forests and other kinds of vegetation that provide effective barriers protecting coastal regions against natural phenomena such as tsunamis, storm surges, and high waves. Combined with chronic climate change events, these

immediate human effects will result in serious and long-term destruction of entire coastal ecosystems (Klemas, 2011). Investigating feature coastal changes is therefore a crucial task for identifying potential factors that can trigger the degradation of a coastal ecosystem. However, in-situ field investigations can be costly and time-consuming, and are almost impossible for a multi-decadal assessment. Alternatively, remotely sensed data can be used to map coastal land cover and often produce reliable results compared to the ground-survey method (Kirui et al., 2013). The freely available Landsat images are widely used to study coastal environments, including habitat mapping and coastline change assessments (e.g., Rokni et al., 2014; Santos et al., 2014; Cardoso et al., 2013; Niya et al., 2013). Moreover, the availability of high-resolution Google Earth Images (GEIs) in recent years has attracted researchers to explore their potential use either as reference information to improve image classification results or as input data to produce high-accuracy classification images for both large- and small-scale study sites. For instance, Gong et al. (2010) used GEIs, containing only three bands (red, green, and blue), and the relevant visualization tools to locate marshland for wetland mapping across the whole of China. Hu et al. (2013) conducted a comparison study to assess the ability of premium GEIs to map the land cover of a regional-scale study site, and found that the classified image produced from GEIs was comparable to that produced from the original QuickBird image. Similarly, a recent study by Collin et al. (2014) investigated the potential of GEIs for bathymetry and coastal habitat mapping on very fine spatial scale (i.e., 0.6 m). Interestingly, they found that the bathymetry map derived from GEIs and the original QuickBird imagery were comparable, and in some cases GEIs can even produce better results. According to these studies, the integrated use of high-resolution GEIs with other remotely sensed data can effectively increase the capacity of remote sensing applications in the environmental study without increasing the financial requirements. For this reason, it would be worth investigating the feasibility of using GEIs together with Landsat data to detect changes in coastal features.

In this study, GEIs and Landsat data were integrated to identify the evolution of coastal features in the KienGiang province in the north-westernmost part of the Mekong Delta. The specific objectives of the study were (i) to delineate and detect the inter-decadal shoreline evolution based on Landsat data; (ii) to detect coastal land cover changes using Landsat data and GEIs; and (iii) to evaluate the impacts of socio-economic activities on the coastal ecosystem, particularly the mangrove ecosystem along the coast of the study area.

2 MATERIALS AND METHODS

2.1 Study Area

This study was conducted in KienGiang province, located in the north-westernmost part of the Mekong Delta, centered on $10^{\circ}4'0.89''$ N and $105^{\circ}1'29''$ E. The study site sits on an 113 km coastal strip, which encompasses about 1780 km² of the KienGiang coastal zone (Fig. 1). The average elevation of this coastal region is relatively low, ranging between 0.2–0.5 m above the mean sea level. This area contains a thin green belt of mangrove forests with poorly constructed dikes at some locations along the shoreline (IUCN, 2013; Duke et al., 2010). Aquaculture, mixed rice–shrimp, paddy, sugarcane, and other crop areas are found in the zone further inland. The low-lying topography compounded by a poor shoreline protection system makes this coastal region very vulnerable to waves and tidal action, although the average wave height and tidal variation in this area are not large (the average wave height is about 0.3 m while the mean tidal range is approximately 0.56 m). As for the rest of the Mekong Delta, the land cover for this area has changed remarkably over the last two decades owing to the economic transition directed by the Vietnam government. Based on the records in Kien Giang province statistical yearbooks, from 1996 to 2013 a large portion of its coastal land was converted into shrimp fields, with the largest changes occurring between 2000 and 2004, from 34.6 thousand hectares to 79.2 thousand hectares. The current socio-economic development of this area is heavily reliant on the agricultural sector (including crop cultivation, livestock, forestry, fishery, and aquaculture production). In 2012, the economic share of this sector alone accounted for 40.02% of the total economic output of the whole province. However, this sector is considered vulnerable to the

effects of climate change, especially in the face of a rising sea level. A study conducted by the Deutsche Gesellschaft für Internationale Zusammenarbeit (GIZ) revealed that the shoreline erosion and accretion in this coastal zone were driven by a natural phenomenon due to the prevalence of the monsoon wind condition and the wave height (GIZ, 2012). Between 2009 and 2010, about 30km of this area’s coastline underwent severe erosion. As a consequence, coastal vegetation, fish ponds, and dyke systems were heavily damaged and 19 coastal villages were directly affected (Duke et al., 2010). In addition to the impact of natural events, anthropogenic activities, improper use of fertilizers and pesticides, and overexploitation of groundwater resources were also major factors that may trigger coastal degradation in this area.

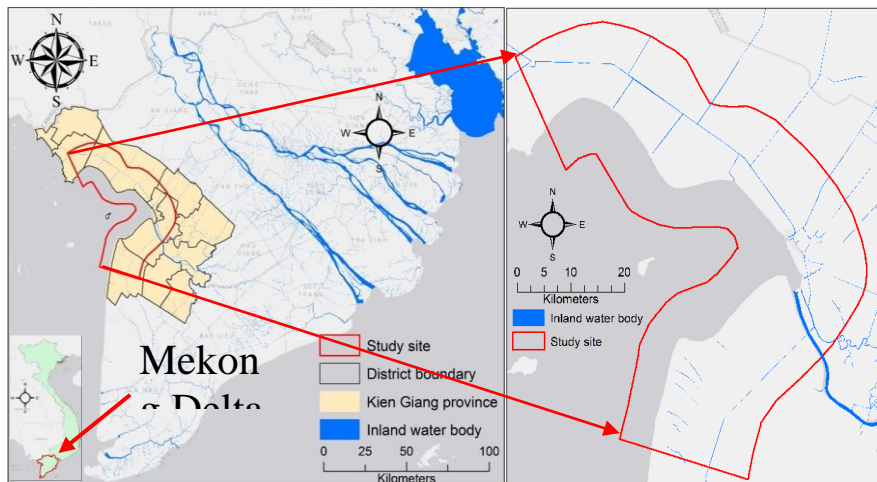


Figure 1. Location map of the study area

2.2 Methodology

The evolution of the shoreline and coastal land cover were investigated for the last two decades based on the analysis of a series of Landsat data and validation with GEIs. To meet the objectives of this study, multiple Landsat images, including Landsat-7 ETM+ and Landsat-5 and -4 TM were used. Moreover, two GEIs acquired on February 21, 2014 were used as reference images for both shoreline delineation and coastal land cover mapping (Fig. 2). The socio-economic information for 1996 and 2000–2013 was extracted from the KienGiang province statistical yearbooks, and the Vietnam statistical yearbooks were also used as ancillary information for assessing the impacts of socio-economic activities

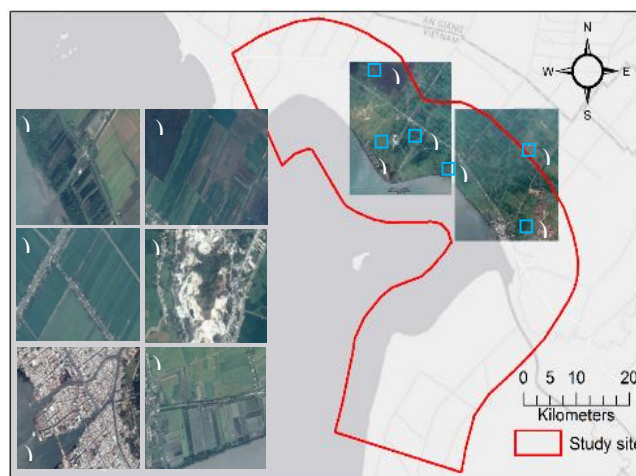


Figure 2. Location map of the two Google Earth images used in this study and close-up visualization of

On coastal habitats in the study area. A summary of the Landsat dataset used in this study is given in Table 1. The detailed methodology for obtaining the GEIs is described in Collin et al. (2014).

Table 1. Summary information of Landsat images used in this study (tide data generated using the NAO.99b system described in Matsumoto et al. (2000))

Images source	Number of bands	Pixel size (m)	Date of acquisition	Acquisition time (GMT)	Tidal status	
					Average high (m)	Stage
Landsat-7 ETM ⁺	9	30 (MS) 15 (PAN)	21-02-2014	03:17:07	-0.070	Fall
Landsat-7 ETM ⁺	9	30 (MS) 15 (PAN)	13-02-2011	03:13:51	-0.207	Fall
Landsat-7 ETM ⁺	9	30 (MS) 15 (PAN)	07-02-2003	03:09:03	-0.012	Rise
Landsat-7 ETM ⁺	9	30 (MS) 15 (PAN)	22-04-2001	03:10:05	-0.059	Fall
Landsat-5 TM	7	30 (MS)	09-02-1995	02:32:01	-0.114	Fall
Landsat-4 TM	7	30 (MS)	05-04-1989	02:53:31	-0.063	Rise
Landsat-4 TM	7	30 (MS)	31-01-1989	02:53:02	-0.150	Fall

2.2.1 Shoreline and Coastal Land Cover Change Detection

The assessment of the shoreline pattern was carried out for the years 1989, 1995, 2001, 2003, 2011, and 2014 based on the analysis of seven Landsat scenes (described in Table 1). In general, an image was used to delineate the shoreline position for one particular year (e.g., the image that was acquired on February 21, 2014 was used to delineate the shoreline position for 2014). However, owing to the presence of clouds that covered some portions of the coastline, two images were combined to generate the entire coastline for the year 1989. The basic technique of this integrated approach is straightforward. First, the cloudy area of an image scene was masked by a simple masking technique. Subsequently, this masked area was replaced by a cloud-free image from another Landsat scene using geo-referenced mosaicking. Similarly, the land cover classification was carried out for only four periods, including 1995, 2001, 2003, and 2014 owing to the limited number of cloud-free images over the study sites. To ensure the accuracy of classification, geometric and radiometric corrections were performed for all images prior to the image classification stage. Moreover, the Landsat image acquired in 2014 was utilized as a base image to perform image-to-image registration for all images. At least 15 ground control points (GCP), which included a road intersect, a waterway, and prominent geomorphological features, were used in this process. A root means square error (RMSE) of less than 0.5 pixels was used as the threshold of acceptable rectification accuracy. In addition, gap filling was also applied on images dated 2003 or later, while cloud masking was performed on the 2001 and 2003 images to remove the very small proportion (less than 1% of the study area) of cloudy areas from the images.

To investigate the spatio-temporal changes of the shoreline pattern, a single band threshold technique was first applied to each Landsat scene to create a binary image revealing the location of the land–water boundary. Then, these land–water boundary images were vectorized and overlaid for further assessment. The spatiotemporal variations of the shoreline pattern, erosion, and accretion rate were then identified based on direct visualization and measurement of the shoreline position in these overlaid images. In this study, the threshold of $b_5=550$ (surface reflectance value of the 5th band) was

identified as the boundary between land and water areas based on direct visualization of each reflectance image.

Coastal habitat mapping was carried out using the maximum likelihood classifier, a supervised classification method focusing on eight major habitats including water surfaces; bare land; urban areas; muddy, rocky, and sandy land; mangrove areas; paddy areas; inundated vegetation (indicated as mangrove–shrimp or rice–shrimp areas), and other vegetation areas. Using GEIs as the ground-truth dataset, 350 pixels were randomly selected from Landsat images for each type of habitat, and 70% of these pixels were used as input points to train the maximum likelihood classifier, with the remaining 30% used to validate the classification results, which were based on the confusion matrix technique. The selection of the training pixels is one of the most important steps in image classification, and it can positively or negatively affect classification results. A set of good training pixels should be pure enough to represent only one class and should be well distributed across the whole image to capture the maximum variation within a particular class. However, it is difficult to meet these criteria, especially when the study area is characterized by highly heterogeneous habitats that may appear as small patches amongst larger areas. To overcome this problem, ISODATA, an unsupervised classification method, was applied to all images prior to the selection of the training pixels to identify the dominant area for each class. The training pixels were then randomly selected based on this unsupervised class image and labeled according to the reference GEI.

All the procedures of satellite image analysis in this study were carried out using the available tools in the ENVI software version 5.0.

2.2.2 Assessment of Anthropogenic Impacts on Coastal Habitats

The impacts of the anthropogenic pressures on coastal habitats, such as the mangrove area, were identified by an exploratory statistical method: Multiple Factor Analysis (MFA). Utilizing MFA, the impacts of various socio-economic indicators on mangrove forests can be numerically and graphically interpreted. In this study, two groups of socio-economic indicators were employed as input data for MFA to reveal the effects of human-driven pressures on the extent of the mangrove area. The first group contained information on the 8 land cover types extracted from the land cover mapping results for the years 1995, 2001, 2003, and 2014, plus the aquaculture breeding area obtained from the statistical yearbooks of Vietnam and Kien Giang province. The second group comprised annual data on the population density and some economic outputs such as aquaculture production, paddy production, and gross output of the industrial sector for six districts located in the study area (See Fig. 1). This district-level dataset was used in this study instead of a dataset covering the exact study area owing to the lack of available information at finer spatial scales. Given that the economic activities in this study area are concentrated along the coastline, the impact of the spatial mismatch of the above-mentioned socio-economic data is not significant. Furthermore, for similar reasons, the data associated with the years 1995 and 2001 were replaced by the data for the years 1996 and 2000, respectively. MFA was carried out using XLSTAT, an add-in tool in Microsoft Excel.

3 RESULTS AND DISCUSSION

3.1 Variation of the Shoreline Pattern

Given that all the Landsat images used for this analysis were acquired during the same season (dry), and the variations in tide levels between each image acquisition period were not significant (Table 1), the effect of tide on the position of delineated shorelines was not taken into account in this study.

The results of the shoreline pattern analysis revealed that from 1989 to the present day, the coastline of the study area has substantially changed; both erosion and accretion were identified. In general, the erosion occurred on the northern and southern coasts of the study site, while the central coastline was relatively stable, except for a coastal protrusion at the southern section where significant accretion was observed (Fig. 3). Moreover, the rates of erosion and accretion were spatially and temporally different.

The average erosion rate from 1989 to 2014 was 9.5m year^{-1} with an extreme erosion rate of 44.5m year^{-1} appearing between 1989 and 1995 in the northern dominant erosion zone (zone (i) in Fig.3). The annual erosion rates in zones (i) and (ii) in Fig. Three during 1995–2001, 2001–2003, and 2011–2014 were approximately 12.5, 22.5, and 28m year^{-1} , respectively. This increasing trend, especially the surge in the erosion rate during 2001–2003, probably resulted from the rapid land cover conversion that occurred during this period due to a boom in aquaculture production. As for the variation in the erosion rate, the spatial and temporal distributions of the erosion pattern along the entire coastline were variable. From 1989 to 2014, the dominant erosion zone shifted from north to south. Remarkably, from 1989 to 2001, coastal erosion was more prevalent in the northern part (Fig. 4 (a)), while from 2001 onward, it was more prevalent in the southern part of the coastline (Fig. 4 (b)), adjacent to the area where coastal land was rapidly being invaded by shrimp breeding activities after the economic reform of the Vietnam government in the early 2000s. On the other hand, in the area where accretion occurred (zone (iii) in Fig. 3), the average accretion rate between 1989 and 2014 was

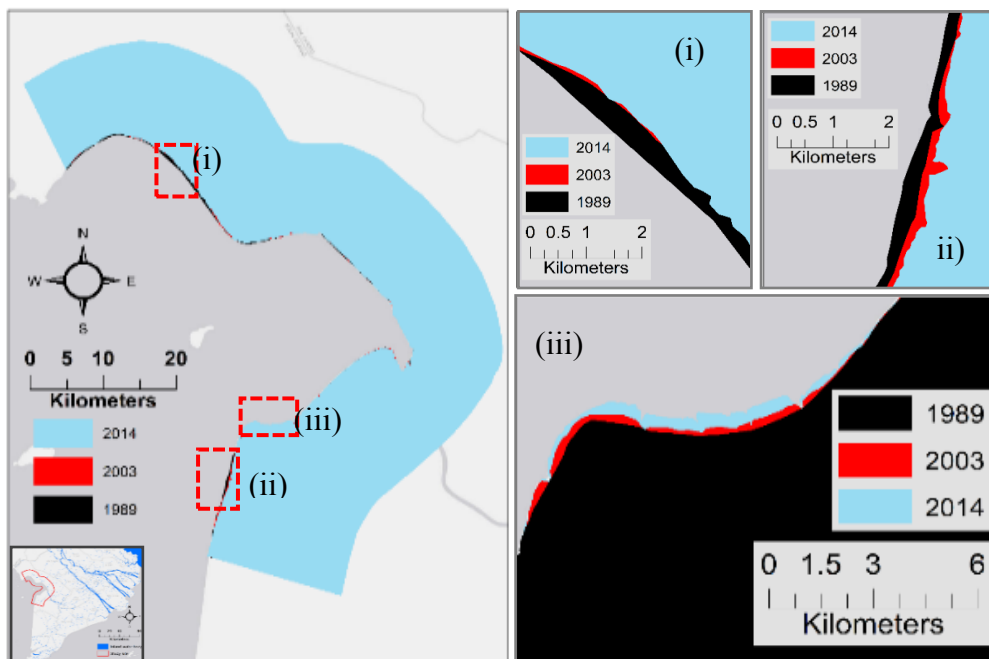


Figure 3. Shoreline erosion and accretion pattern from 1989 to 2014: the dominant erosion zone (i and ii), and the accretion zone (iii)

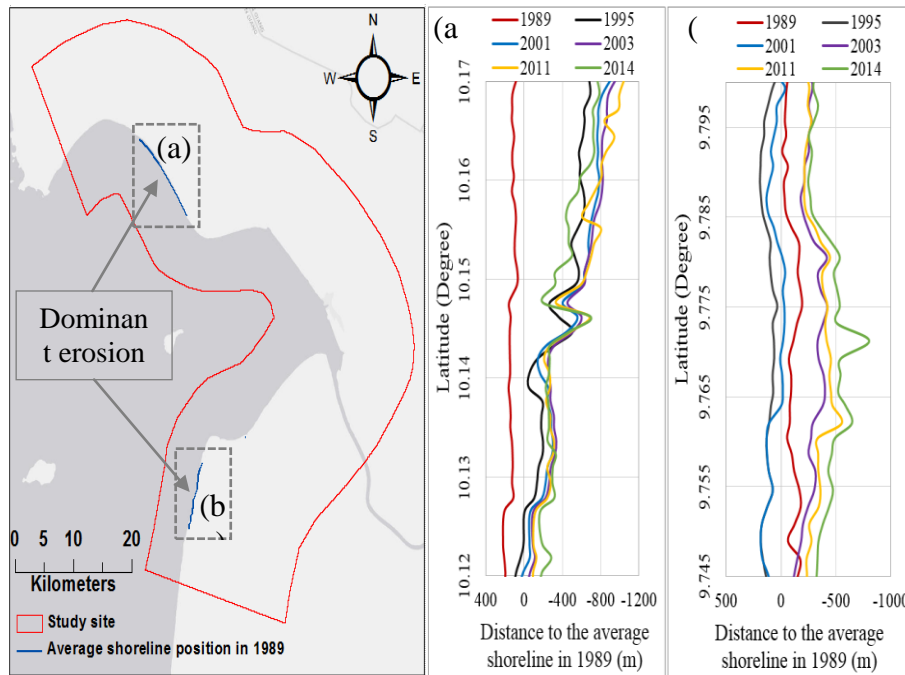


Figure 4. Shoreline pattern variation from 1989 to 2014 at the most dominant erosion sites (negative value indicates erosion): shoreline position at the northern dominant erosion site (a); shoreline position at the southern

With a maximum rate of 47.6m year^{-1} occurring between 1989 and 1995. The accretion rates during 1995–2001 and 2011–2014 were 13m year^{-1} and 11.5m year^{-1} , respectively. No accretion occurred during 2000–2003; conversely, an abrupt increase in coastal erosion was found during this period. It is important to notice that the accretion area was located near the southern dominant erosion zone (Fig. 3) and also bordered the area where the coastal land cover was severely altered by aquaculture activities. It can, therefore, be inferred that land cover conversions into aquaculture farms during 2000–2003 had significant adverse effects on coastal erosion in the study area. Furthermore, according to the results of a study conducted by Duke et al. (2010), the erosion rate in some areas along the KienGiang coastline reached 24m year^{-1} during 2009–2010. This finding, combined with the results of our current study, may indicate that the shoreline erosion in the KienGiang province is severe and constantly worsening. Moreover, although the erosion phenomenon in this area is considered a natural event (GIZ, 2012), its increasing intensity is driven by anthropogenic pressures, particularly the massive changes in the coastal land use that occurred between 2000 and 2003. Furthermore, these human impacts have remained unchanged regardless of the coastal protection programs that have been conducted in recent years (e.g., construction of sea dykes, artificial protecting fences, and replanting of the mangrove forest under the GTZ KienGiang Biosphere Reserve Project).

3.2 Coastal Land Cover Changes

Using a representative training data set, the maximum likelihood classifier provided satisfactory classification results. The overall classification accuracy and Kappa coefficient were 86.67% and 0.85, 81.87% and 0.79, 93.65% and 0.92, and 90.33% and 0.89 for 2014, 2003, 2001, and 1995, respectively. The classified maps are presented in Fig.5. Based on these classification results, the land cover in the study area changed significantly between 1995 and 2014. Table 2 provides a summary of these results. In 1995, vegetation (i.e., vegetation areas other than paddy and mangrove areas), bare land, and Paddy areas were found to be the most common land cover type in the study site, whereas in 2014, paddy fields became the dominant land use, followed by other vegetation, inland water surfaces, and other land cover types. The bare land area accounted for 34.17% of the total land area in 1995 and successively declined to 7.28% in 2014. For all cases, the bare land area was not prevalent in the middle part of the study site where most of the land area was covered by paddy fields, except in 2001 (Fig. 5).

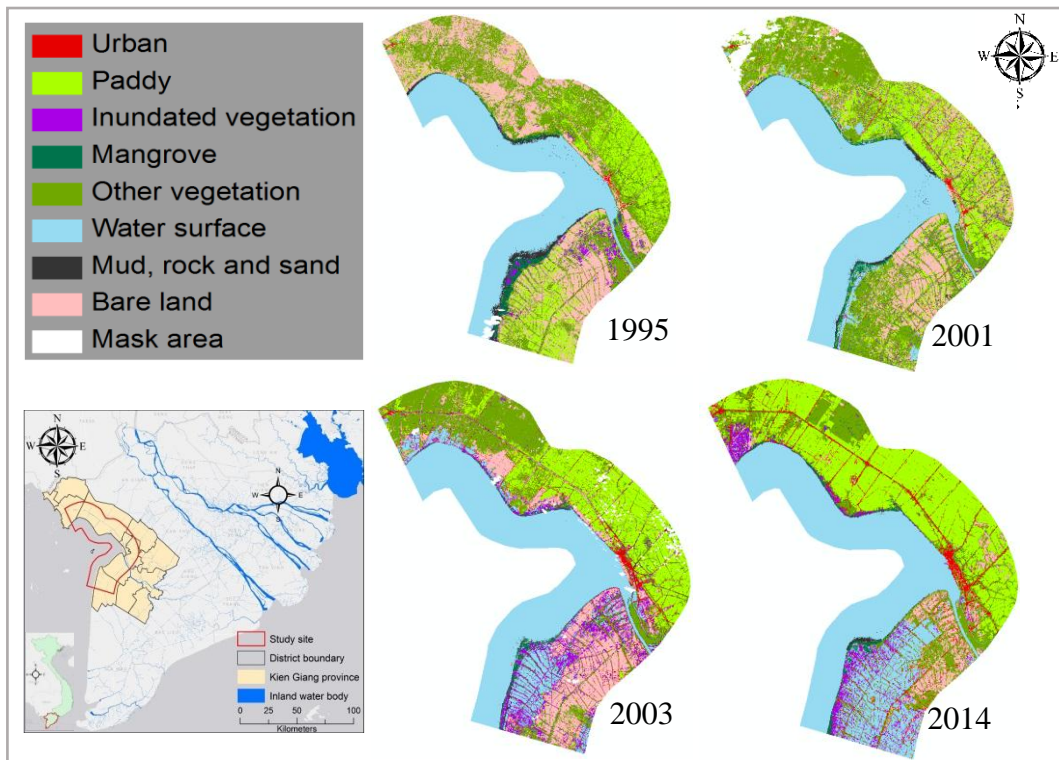


Figure 5. Classification results of the coastal land cover of the study site in 1995, 2001, 2003 and 2014

This exceptional year can be explained by the inconsistent acquisition date of the input Landsat images used in this study (see Table 1). Regarding 1995, 2003, and 2014, the selected images were acquired during early to mid-February, which is the first half of the dry season. In contrast, the input image for 2001 was acquired in late April, the end of the dry season when most crops (paddy fields) may have already been harvested, and the soil dryness has become more pronounced. The paddy area increased from 18.84% in 1995 to 28.68% in 2001, then dropped to 25.21% in 2003 and peaked again at 41% in 2014. As for the paddy area variation trend, the areas of inland water surfaces and inundated vegetation, which are related to aquaculture production, increased significantly between 1995 and 2014. The area of inland water surfaces increased from 0.32% in 1995 to 14.84% in 2014, while the inundated vegetation area increased from 2.42% in 1995 to 6.07% in 2014. More interestingly, the variation trend of the inland water surfaces appeared as an abrupt jump between 2001 and 2003 (from 3.68% to 9.14%), indicating that rapid land cover conversions into aquaculture ponds happened during this period. These results closely match the variation trend for the aquaculture production area retrieved from the statistical yearbooks of Kien Giang province (Fig. 6). On the other hand, during this period the paddy area dropped remarkably. This can be explained by the socio-economic activities, which changed from rice-oriented to aquaculture-oriented between 2001 and 2003.

Table 2. Percentage of each land cover type compared with the total area of the study site in 1995, 2001, 2003 and 2014

Land Cover	1995	2001	2003	2014
Urban	0.74%	1.41%	4.22%	6.35%
Paddy	18.84%	28.68%	25.21%	41.00%
Mangrove	3.61%	3.13%	2.43%	2.05%
Inundated vegetation	2.42%	5.26%	9.63%	6.07%
Other vegetation	37.20%	38.02%	27.40%	21.14%
Inland water	0.32%	3.68%	9.14%	14.84%
Mud, rock, and sand	2.69%	1.48%	2.29%	1.27%
Bare land	34.17%	18.34%	19.67%	7.28%

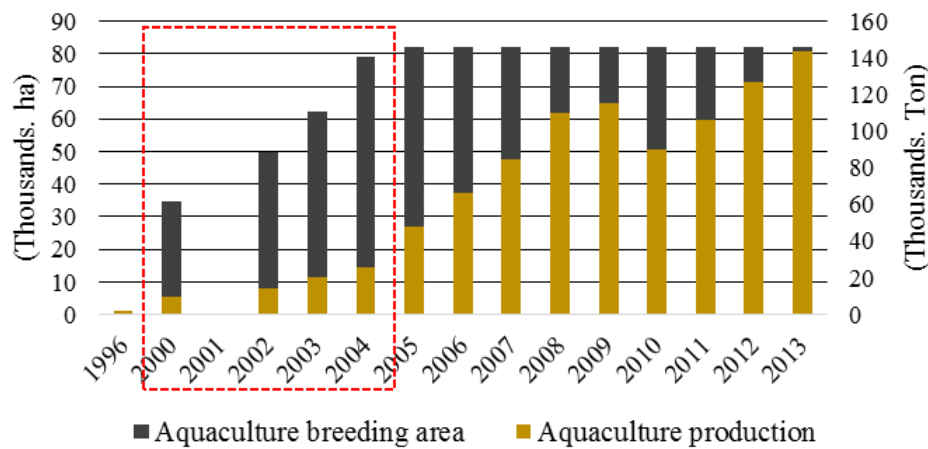


Figure 6. Change in aquaculture breeding area and production in Kien Giang province from 1996 to 2013

The mangrove area declined significantly between 1995 and 2014. It accounted for 3.61% of the total land area in 1995 and dropped to 3.13% in 2001, 2.43% in 2003, and 2.05% in 2014. In general, the average rate of mangrove loss between 1995 and 2014 was about 2.29% of the total mangrove area per year. This rate of decline is relatively high, and could, if this trend persists, lead to complete elimination of the mangrove forests from the coastline of the study area within 25 years. This continuous loss of the mangrove area mainly resulted from the conversion of the land use along the coastline, which can be seen clearly in Fig. 7. Moreover, between 2001 and 2003, the rate of mangrove loss was as high as 11.16% of the total mangrove area per year. This rapid loss of the mangrove forest coincided with the rapid increase of inland water surfaces and aquaculture areas (Fig. 6), indicating the direct impact of aquaculture development on the degradation of the mangrove forest in this coastal zone. Aside from these human impacts, natural events such as severe coastal erosion may also further trigger the destruction of the mangrove forests along the shoreline. As identified in this study, the area of mud, rock, and sand that generally appeared adjacent to the mangrove dominated zone (Fig. 5 and 7) had a similar variation trend to that of the mangrove area in that it continuously and significantly declined from 1995 onward. Its area was about 2.69% of the total land area in 1995, dropping to 1.27% in 2014. This similarity in the variation patterns clearly indicates that either the degradation of mangrove area triggered the coastal erosion episode or vice versa.

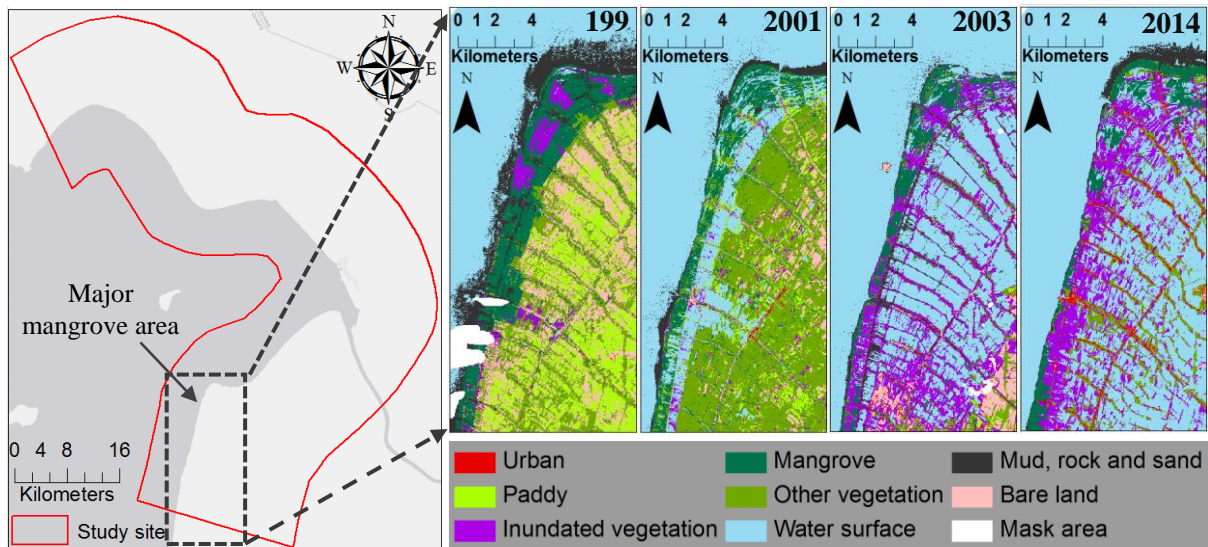


Figure 7. Change in mangrove area and adjacent land use from 1995 to 2014 in the mangrove dominated zone

3.3 Anthropogenic Impacts on Coastal Habitats

Figure 8 shows biplot graph of the MFA results, which depict the relationships between the variation of the mangrove area and some major economic indicators. It displays all variables synoptically with their corresponding factor loading (i.e., the correlation of a variable with a factor). The first two factors (F1 and F2) accounted for 93.36% of the total data variability. Highly correlated variables would appear close to each other on the biplot graph, meaning that they have a similar correlation level with the same factor.

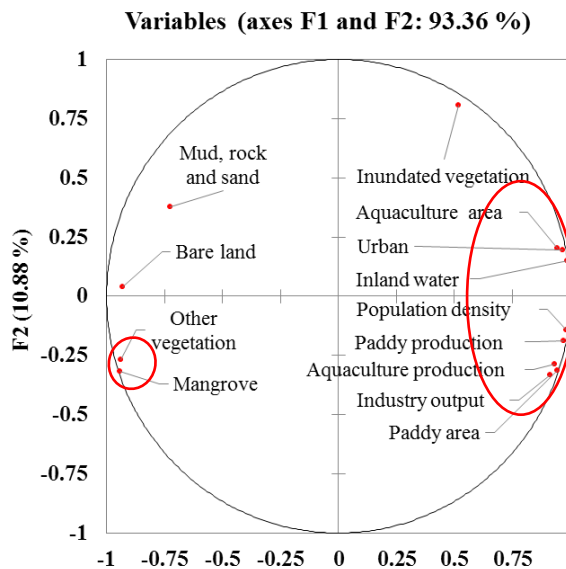


Figure 8. Biplot graph showing the relationship between the mangrove area and major socio-economic indicators

According to the results shown in Fig. 8, it is obvious that the mangrove area is strongly and negatively correlated with other types of land cover including urban areas, inland water surfaces, aquaculture areas, and inundated vegetation and paddy areas. The correlation coefficients between the mangrove area and these land cover types were -0.95 , -0.97 , -0.92 , -0.77 , and -0.82 (with $\alpha=0.05$ significance level), respectively. Likewise, other socio-economic indicators, such as the

population density, paddy production, aquaculture production, and the gross output of the industrial sector, were also negatively and significantly correlated with the extent of the mangrove area, with correlation coefficients of -0.89 , -0.84 , -0.79 , and -0.72 (all with a $p = 0.05$ significance level), respectively. Based on these results, the increase of inland water surfaces (probably due to the increase in aquaculture breeding areas) was the main driver leading to mangrove ecosystem degradation in this study area. The other major drivers were the urban area, the aquaculture area, the population density, paddy production, and the paddy area. Interestingly, the paddy area seemed to have fewer adverse effects on the extent of the mangrove area compared with paddy production. This indicates that agricultural activities may indirectly affect the mangrove ecosystem, with the most destructive effects stemming from the increasing pollution load due to intensive farming practices. In contrast, the aquaculture area had a more pronounced effect on the reduction of the mangrove area compared with aquaculture production, revealing the direct impact of land reclamation for aquaculture activities on the degradation of the mangrove forest along the coastline of this study area.

Based on the above results, it can be concluded that the land cover conversion due to socio-economic activities has triggered a remarkable decline in the mangrove area in the study region. Furthermore, intensive activities tended to increase production rates, such as the aquaculture and paddy production rates; combined with an increasing number of human inhabitants, these increases can further exacerbate the mangrove decline.

4 CONCLUSIONS

From 1989 to 2014, the shoreline pattern of the study area changed significantly owing to erosion and accretion phenomena, which were intensified by concentrated human activities along the coastline, especially the conversion of coastal land into aquaculture ponds between 2000 and 2003. The rate of coastal erosion increased continuously up to the present day, with the dominant erosion zone shifting from north to south. Also, the coastal land cover has significantly changed over the same period. The area covered by bare surfaces decreased significantly while other land cover types, such as the urban areas, vegetation cover, and inland water surfaces, have continuously increased. This finding reflects the trend of increasing human activity in this coastal region. Moreover, the contrasting variation patterns of the paddy area and inland water surface show that the socio-economic situation in the study area changed from rice-oriented to aquaculture-oriented, with the most dramatic changes occurring in the early 2000s. The extent of the mangrove forest has continuously declined from 1995 onward. The conversion of coastal land cover due to socio-economic development activities in the area was found to have potentially negative effects on the degradation of the mangrove area. Moreover, concentrated economic activities such as intensive shrimp breeding and rice cultivation, industrial development, and the increasing number of human inhabitants can result in more severe damage to the mangrove ecosystem. Although some programs aiming to protect the mangrove forests have been conducted in this coastal zone, these policies seem to be ineffective at preventing the degradation of the mangrove ecosystem.

ACKNOWLEDGMENTS

This study was supported by the ASEAN University Network of Southeast Asia Engineering Education Development Network Project (AUN/SEED-Net) JICA program and the Japan Society for Promotion of Science (JSPS) Core-to-Core Program (B. Asia-Africa Science Platforms), a Grant-in-Aid for JSPS Fellows (No. 2402800), and a Grant-in-Aid for Scientific Research (A) (No. 24246086 and 25257305) from the JSPS.

REFERENCES

- Cardoso, F.G., Jr, S.C. & Souza-Filho, M.W.P. (2013) Using spectral analysis of Landsat-5 TM images to map coastal wetlands in the Amazon River mouth, Brazil. *Wetland Ecology and Management*, 22 (1), pp.79-92. Doi:10.1007/s11273-013-9324-4.

Collin, A., Nadaoka, K., & Nakamura, T. (2014) Mapping VHR Water Depth, Seabed and Land Cover Using Google Earth Data. *ISPRS International Journal of Geo-Information*, 3(4), pp.1157–1179. doi:10.3390/ijgi3041157.

Duke, N., Wilson, N., Mackenzie, J., Nguyen, H. H. & Puller, D. (2010). Assessing Mangrove Forests, Shoreline Condition and Feasibility of REDD for KienGiang Province Vietnam. GTZ KienGiang Biosphere Reserve Project, Technical Report

GIZ (2012) Coastal Rehabilitation and Mangrove Restoration using Melaleuca Fences, Practical Experience from KienGiang Province. GTZ KienGiang Biosphere Reserve Project, Technical Report.

Gong, P., Niu, Z., Cheng, X., Zhao, K., Zhou, D., Guo, J., Liang, L., Wang, X., Li, D., Huang, H., Wang, Y., Wang, K., Li, W., Wang X., Ying, Q., Yang, Z. Z., Ye, Y., Li, Z., Zhuang, D., Chi, Y., Zhou, H. & Yan, J. (2010) China's wetland change (1990–2000) determined by remote sensing. *Science China Earth Science*, 53 (7), pp.1036–1042. doi:10.1007/s11430-010-4002-3.

Hu, Q., Wu, W., Xia, T., Yu, Q., Yang, P., Li, Z., Song, Q. (2013) Exploring the use of Google Earth imagery and object-based methods in land use/cover mapping. *Remote Sensing*, 5, pp.6026–6042. doi:10.3390/rs5116026.

IUCN. (2013). Building Resilience to Climate Change Impacts □ : Coastal Southeast Asia KienGiang Province, Viet Nam. Factsheet.

Kirui, K. B., Kairo, J. G., Bosire, J., Viergever, K. M., Rudra, S., Huxham, M., & Briers, R. a. (2013) Mapping of mangrove forest land cover change along the Kenya coastline using Landsat imagery. *Ocean & Coastal Management*, 83, pp.19–24. doi:10.1016/j.ocecoaman.2011.12.004.

Klemas, V. (2011) Remote sensing techniques for studying coastal ecosystems: an overview. *Coastal Research*, 27(1), pp.2-17. West Palm Beach (Florida).

Manson, F.J., Loneragan, N.R., Skilleter, G.A. & Phinn, S.R. (2005) An evaluation of the evidence for linkages between mangroves and fisheries: a synthesis of the literature and identification of research directions. *Oceanography and Marine Biology-An Annual Review*, 43, pp. 483-513.

Matsumoto, K., Takanezawa, T. & Ooe, M. (2000) Ocean Tide Models Developed by Assimilating TOPEX/POSEIDON Altimeter Data into Hydrodynamical Model: A Global Model and a Regional Model Around Japan, *Journal of Oceanography*, 56, pp. 567-581.

Nagelkerken, I., Blaber, S. J. M., Bouillon, S., Green, P., Haywood, M., Kirton, L. G., & Somerfield, P. J. (2008) The habitat function of mangroves for terrestrial and marine fauna: A review. *Aquatic Botany*, 89(2), pp. 155–185. doi:10.1016/j.aquabot.2007.12.007.

Niya, K.A., Alesheikh, A.A., Soltanpor, M. & Kheirkhahzarkesh, M.M. (2013) Shoreline change mapping using remote sensing and GIS. *Remote Sensing Applications*, 3(3).

Rokni, K., Ahmad, A., Selamat, A. & Hazini, S. (2014) Water feature extraction and change detection using multi-temporal Landsat imagery. *Remote Sensing*, 6, pp. 4173-4189, doi: 10.3390/rs6054173.

Santos, L. C. M., Matos, H. R., Schaeffer-Novelli, Y., Cunha-Lignon, M., Bitencourt, M. D., Koedam, N., & Dahdouh-Guebas, F. (2014) Anthropogenic activities on mangrove areas (São Francisco River Estuary, Brazil Northeast): A GIS-based analysis of CBERS and SPOT images to aid in local management. *Ocean & Coastal Management*, 89, pp. 39–50. doi:10.1016/j.ocecoaman.2013.12.010.